Colour polymorphism associated with a gene duplication in male wood tiger moths

Melanie N. Brien[1*†], Anna Orteu[2*], Eugenie C. Yen[2], Juan A. Galarza[1,3], Jimi Kirvesoja[3], Hannu Pakkanen[4], Kazumasa Wakamatsu[5], Chris D. Jiggins[2**], Johanna Mappes[1,3**].

[1]*Organismal and Evolutionary Biology Research Program, Faculty of Biological and Environmental Sciences, University of Helsinki, Finland.*

[2]*Department of Zoology, University of Cambridge, United Kingdom.*

[3]*Department of Biological and Environmental Science, University of Jyväskylä, Finland.*

[4]*Department of Chemistry, University of Jyväskylä, Finland.*

[5]*Institute for Melanin Chemistry, Fujita Health University, Toyoake, Japan.*

*Co-first authors.

**Co-senior authors.

†Correspondence: mnbrien1@gmail.com

Abstract

Colour is often used as an aposematic warning signal, with predator learning expected to lead to a single colour pattern within a population. However, there are many puzzling cases where aposematic signals are also polymorphic. The wood tiger moth, *Arctia plantaginis*, displays bright hindwing colours associated with unpalatability, and males have discrete colour morphs which vary in frequency between localities. In Finland, both white and yellow morphs can be found, and these colour morphs also differ in behavioural and life-history traits. Here, we show that male colour is linked to an extra copy of a *yellow* family gene that is only present in the white morphs. This white-specific duplication, which we name *valkea,* is highly upregulated during wing development, and CRISPR knockouts validate the role of *valkea* in producing white wing colour. We also characterise the pigments responsible for yellow, white and black colouration, showing that yellow is partly produced by pheomelanins, while black is dopamine-derived eumelanin. Our results add to a growing number of studies on the genetic architecture of complex and seemingly paradoxical polymorphisms, and the role of gene duplications and structural variation in adaptive evolution.

Introduction

Colour polymorphisms, defined as the presence of multiple discrete colour phenotypes within a population (Huxley, 1955), provide an ideal trait to study natural and sexual selection. Colour phenotypes can have an effect on fitness in many contexts including camouflage, mimicry and mating success. Colour is often associated with aposematism, where it acts as a signal, warning predators of unpalatability (Cott, 1940; Cuthill *et al.*, 2017). In such cases, predator learning should favour the most common colour pattern, leading to positive frequency dependent selection (Endler, 1988). Despite this, aposematic polymorphisms can be stable when selection is context-dependent (Briolat *et al.*, 2019), especially where genetic correlations between colour phenotypes and other traits lead to complex fitness landscapes (reviewed by McKinnon and Pierotti, 2010).

A variety of genetic mechanisms can underpin these types of complex polymorphisms involving multiple associated traits (Orteu and Jiggins, 2020). In many cases, such complex polymorphisms are controlled by 'supergenes' in which divergent alleles at several linked genes are maintained in strong linkage disequilibrium by reduced recombination. The most common mechanism for locally reduced recombination are inversions, which range from single inversions involving a small number of genes, to multiple nested inversions covering large genomic regions (Joron *et al.*, 2011; Wang *et al.*, 2013; Küpper *et al.*, 2016; Funk *et al.*, 2021). Nonetheless, other mechanisms for reducing recombination, such as centromeres or large genomic deletions, may also play a role. An alternative mechanism is that a single regulatory gene controls variation via multiple downstream effects (Thompson and Jiggins, 2014). While there are fewer instances in which multiple phenotypes seem to be controlled by a single gene, one potential example is the common wall lizard, where colour genes have pleiotropic effects on behavioural and reproductive traits (Andrade *et al.*, 2019). Multiple mutations within a single gene can also lead to variation in multiple traits (Linnen *et al.*, 2013).

The wood tiger moth, *Arctia plantaginis,* has a complex polymorphism that has been well studied in an ecological context. Males show polymorphic aposematic hindwing colouration with discrete yellow, white or red hindwing colour morphs found at varying frequencies in different geographic locations. In Finland, for example, both yellow and white morphs can be found, with white morphs varying in frequency from 40 to 75% (Galarza *et al.*, 2014). In Estonia, white morphs make up 97% of the population, while yellows morphs form a

completely monomorphic population in Scotland (Hegna, Galarza and Mappes, 2015) (Figure 1). Long term breeding studies of these moths have shown that male hindwing colour is a Mendelian trait controlled by a single locus with two alleles (Suomalainen, 1938; Nokelainen *et al.*, 2022). White alleles (W) are dominant over the yellow (y). These colour genotypes also covary with behavioural and life-history traits, contributing to the maintenance of this polymorphism. Yellow males are subject to lower levels of predation in the wild (Nokelainen *et al.*, 2012, 2014), while white males have a positive frequency-dependent mating advantage (Gordon *et al.*, 2015). There are differences in chemical defences, and bird reactions to these defences, between the genotypes (Rojas *et al.*, 2017; Winters *et al.*, 2021). Yellow morphs show reduced flight activity compared to white males, although yellows may fly at more selective times, i.e. at peak female calling periods (Rojas, Gordon and Mappes, 2015). Increased reproductive success in Wy genotype females points towards strong heterozygote advantage (De Pasqual *et al.*, 2022). In summary, there is a trade-off between natural selection through predation and reproductive success, which contributes to the maintenance of this polymorphism (Rönkä *et al.*, 2020).

Despite the large body of research on *A. plantaginis* colour morphs, the genetic basis of this polymorphism is unknown. Here, we explore male hindwing colour variation using linkage mapping, whole genome data and gene expression analyses, with wild populations and lab crosses, to identify the locus controlling the colour polymorphism. We use CRISPR/Cas9 gene knockouts to determine the function of the identified gene, and then characterise the pigments producing yellow, white, and black colouration on the wings of male *A. plantaginis*. Our findings aim to provide an example of the genetic architecture controlling a trait that is part of a complex polymorphism.

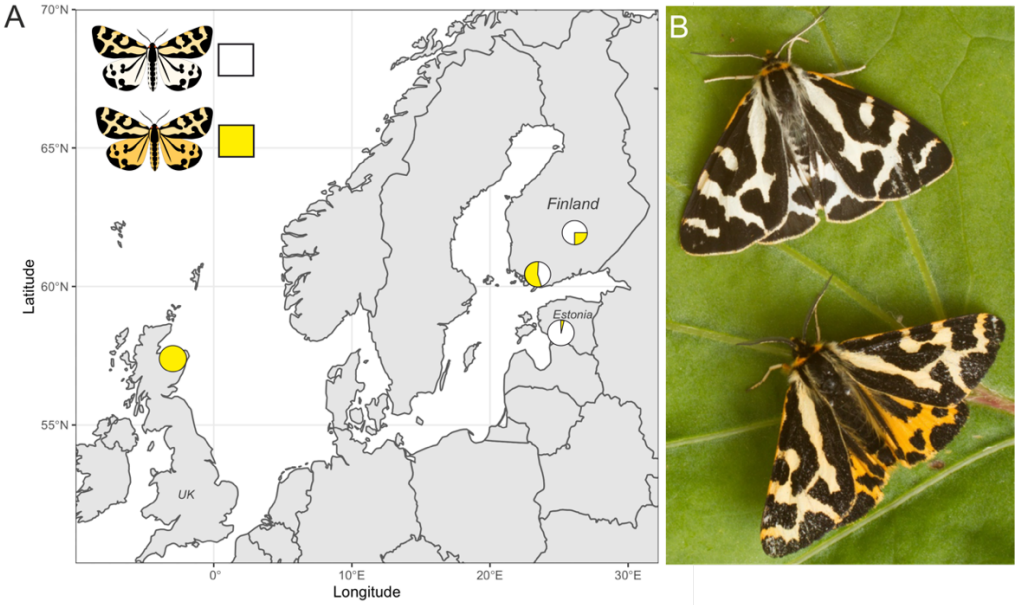

Figure 1: (A) Sampling locations and frequencies of yellow and white *Arctia plantaginis* males in Finland, Scotland and Estonia. (B) Males of the white and yellow colour morphs (Credit: Samuel Waldron).

Results

A narrow genomic region is associated with hindwing colour

To investigate the genetic basis of male hindwing colouration in *A. plantaginis*, we carried out a quantitative trait locus (QTL) mapping analysis using crosses between heterozygous Wy males and homozygous yy females. We used RADseq data aligned to the yellow *A. plantaginis* reference genome from 172 male offspring (90 white and 82 yellow) from four families. The QTL analysis identified a single marker associated with male hindwing colour (Figure 2A). This marker was found on scaffold YY_tarseq_206_arrow at position 9,887,968bp (95% confidence intervals 9,349,978-9,888,009bp) and had a LOD score of 32.8 ($p<0.001$). The significant marker explains around 75% of the phenotypic variation and, with one exception, yellow individuals all had a homozygous yy genotype at this marker.

To further narrow down this region, we ran a genome wide association study (GWAS) using whole genome sequences of males from four populations: polymorphic Southern Finland (5 white, 5 yellow) and Central Finland (10 white, 10 yellow), Estonia (4 white), where males are mostly white, and monomorphic Scotland (12 yellow), where all males are yellow. This identified a region of associated SNPs also on scaffold 206 (Figure 2B). Two SNPs, 137bp apart (at positions 9,885,384 and 9,885,521), were significant above a strict Bonferroni

corrected threshold. 162 SNPs were over the threshold of p<0.0001 and, of these, 155 are within a 99kb region on scaffold 206 (9,833,387-9,932,264bp). The top SNPs are within 2.5kb from the top QTL marker, and the SNP at this marker has a p-value <0.0001.

The 538Kb QTL interval contains 21 genes (Table S1) which were annotated with reference to *D. melanogaster*. Of these genes, four are part of the *yellow* gene family. The top two SNPs from the GWAS, and the top marker from the QTL, fall in a non-coding region upstream of the gene, *yellow-e*, and are also close to an additional *yellow* gene, *yellow-g.*

Identifying structural variation in this region

The trio binning method used by Yen et al. (2020) to assemble the *A. plantaginis* reference genome produced two reference sequences, one for a white allele and one for a yellow allele. We extracted the region containing the QTL interval from the yellow reference and aligned it against the white reference. The alignment showed a duplicated region approximately 117kb long on scaffold 419 of the white reference from around 6,941,000-7,058,000bp (Figure 2 - figure supplement 1). The *yellow-e* gene and its flanking regions are within this sequence and are therefore duplicated in the white reference (Figure 2C). One copy of the gene (named jg1310 in the W annotation) has 7 exons and is similar to the *yellow-e* gene in the yellow reference (99.7% identity in coding sequences). The second copy unique to the white scaffold (jg1308) has only the first 5 exons (81.8% identical to the gene in the yellow reference), possibly due to a stop codon mutation in the 5th exon. For clarity, we named this duplicated white-specific copy *valkea*, in reference to a Finnish word for 'white'. While all white samples had consistent coverage of reads across the duplicated region, coverage was patchy in yellow samples, with many regions having no and very low coverage in yellow samples (Figure 2D). Those reads that map in the *valkea* region in yellow samples are likely to be mapping errors, because the sequence similarity is high and mapping quality is reduced within the duplication (Figure 2 – figure supplement 2). When increasing the mapping quality filtering, read depth decreases more in yellow samples compared to white samples in this region (Figure 2 – figure supplement 3). We confirmed the absence of this region in yellow individuals by designing primers within the duplication (Table S2, Appendix Figure 1), which only amplified in WW and Wy samples, including Finnish, Estonian and lab populations.

141 To confirm that both of these gene copies are related to *yellow-e*, we compared them to
142 *yellow-e* orthologs found in *Bombyx mori*, *Heliconius melpomene* and *Drosophila*
143 *melanogaster,* along with other *yellow* genes from *A. plantaginis* and *B. mori*. Both of the
144 tiger moth genes were most closely related to the *H. melpomene yellow-e* (Figure 2 – figure
145 supplement 4). Between *valkea* and *yellow-e* there is an additional gene which showed
146 highest similarity to *Drosophila yellow-g2* (when extracted from both the white and yellow
147 references). This gene is not part of the duplicated sequence and is present as a single copy in
148 both morphs. Coverage across *yellow-g* and *yellow-e* genome regions in wild samples is
149 similar in both morphs (Figure 2). Upstream of the duplication is an unnamed gene (listed as
150 jg6744 in the yellow annotation and jg1307 in the white). This is the same orthologous gene
151 in both reference genomes, having 99.3% identity. Similarly, if we look at the 150kb
152 upstream region, sequence identity is 99.98%. There are no non-synonymous mutations
153 between coding sequences of *yellow-e* when comparing the white and yellow references,
154 although there are differences in the first exon of *yellow-g*. The absence of this duplicated
155 region in the yellow morphs means we cannot determine if there is a change in linkage
156 disequilibrium across white and yellow morphs.

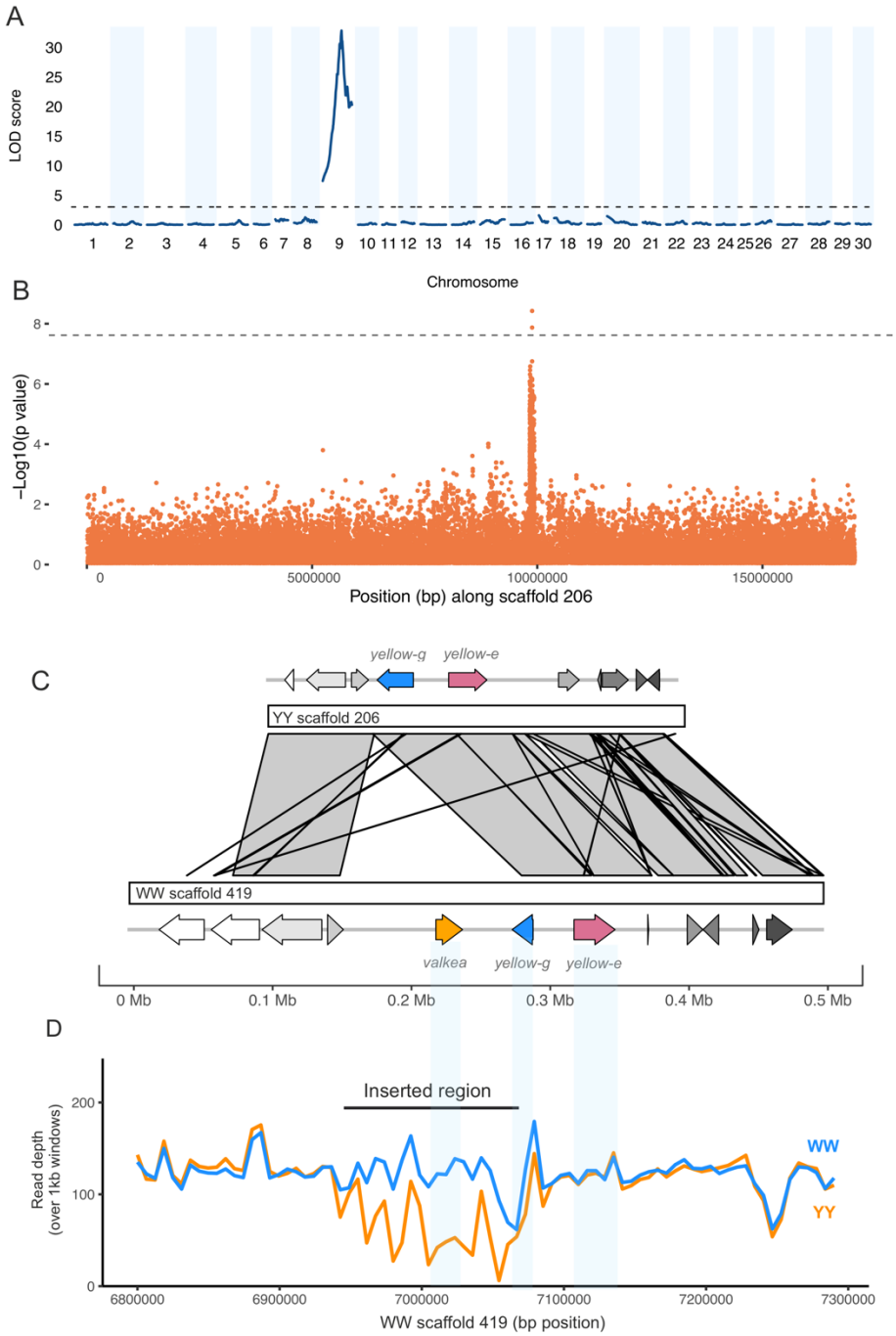

157

158 Figure 2: A duplicated region in white morphs is associated with male hindwing colour. (A) QTL
159 analysis of white and yellow F1 males (n=172) reveals a 500kb region significant on scaffold 206,
160 part of linkage group 9. The dotted line indicates the significance threshold determined by
161 permutation tests (p=0.05). (B) A GWAS of wild samples (n=46) showed SNPs associated with
162 hindwing colour along the same scaffold. The dotted line shows the Bonferroni corrected significance
163 threshold. (C) An insertion in the white reference sequence contains a copy of the *yellow-e* gene,
164 which we named *valkea*, in addition to the *yellow-e* present in both white and yellow morphs. (D)
165 Mean read depth across the candidate region in all Finnish white (WW and Wy) and yellow (yy)
166 samples.

167 *Valkea is differentially expressed between morphs*

168 To pinpoint which of these candidate genes is associated with male wing polymorphism in *A.*
169 *plantaginis,* we next performed gene expression analyses across several developmental
170 stages. Based on knowledge of the expression patterns of *yellow* genes (Ferguson *et al.*,
171 2011) and other melanin pathway genes such as *pale, ebony and ddc* in Lepidoptera (Zhang
172 *et al.*, 2017), we hypothesised that changes in gene regulation that control the development of
173 wing colour morphs in the tiger moth most likely occur during pupal development. Pupal
174 development in the wood tiger moth lasts for approximately 8 days, and no colour is present
175 in the wings until day 7, when the yellow pigment appears. A few hours later, black melanin
176 pigmentation is deposited. We sampled two stages early in development when no colouration
177 is present in the wings (72 hours post-pupation, and 5 day old pupae), and two stages later in
178 development: the point when yellow appears in yy morphs (Pre-mel, 7 day old pupae) and the
179 other after black melanin has also been deposited (Mel, 7-8 days old). Forty individuals were
180 sampled in total - five per genotype and stage.

181 First, we explored the general patterns of expression by mapping RNAseq reads to the white
182 reference genome, which contains the duplicated region that includes *valkea*. We filtered out
183 lowly expressed genes, retaining 10,920 genes and used Multidimensional Scaling (MDS), a
184 dimensionality reduction technique, to explore which factors explain genome-wide variation
185 in gene expression between samples. We observed that samples clustered based on their
186 developmental stage, suggesting it is an important factor driving differences in genome-wide
187 gene expression between samples (Figure 3 – figure supplement 1). Such a pattern would be
188 expected as many genes are involved in development and thus are likely to be differentially
189 expressed (DE) between developmental stages. No apparent clustering can be observed
190 among samples of the same colour morph.

191 We next compared gene expression between yy and WW individuals at each of the
192 developmental stages. Overall, 99 genes were differentially expressed (FDR < 0.05) between
193 the two morphs (Figure 3A). Two of these DE genes, *yellow-e* and *valkea*, are two of the 22
194 genes identified in the GWAS and QTL analysis. *Valkea* was overexpressed in white
195 individuals in the pre-melanin stage with a Log Fold Change of 10.32 and a p-value of 2.18e-
196 06. As *valkea* is only fully present in the W genome, it is not expected to be expressed at all
197 in the Y genome. *Yellow-e* was also overexpressed in white individuals during the pre-
198 melanin stage with a Log Fold Change of 3.86 and adjusted p-value of 5.62e-06. In other

developmental stages, neither *valkea* nor *yellow-e* showed differences in expression between morphs (Figure 3B).

Of the 99 genes differentially expressed between white and yellow individuals across development, 49 were upregulated in the yy morph, while the remaining 50 were upregulated in WW individuals. The earliest developmental stage, 72-hours, was the stage with the highest number of DE genes (n=48), while the 5-day old stage had the fewest (n=7). One gene which encodes a C2H2 zinc finger transcription factor in *D. melanogaster*, '*jg15945*', was over-expressed in yy in the first three stages (Figure 3 – figure supplement 2).

Finally, the GWAS and QTL peaks of association are situated in scaffold 419 of the WW reference assembly, which in a WW linkage map forms a linkage group along with 6 more scaffolds (472, 487, 515, 531, 540 and 609). We found that 12 genes present in this linkage group were differentially expressed, including *valkea* and *yellow-e* (Table S3), and identified their orthologues in *Drosophila melanogaster*.

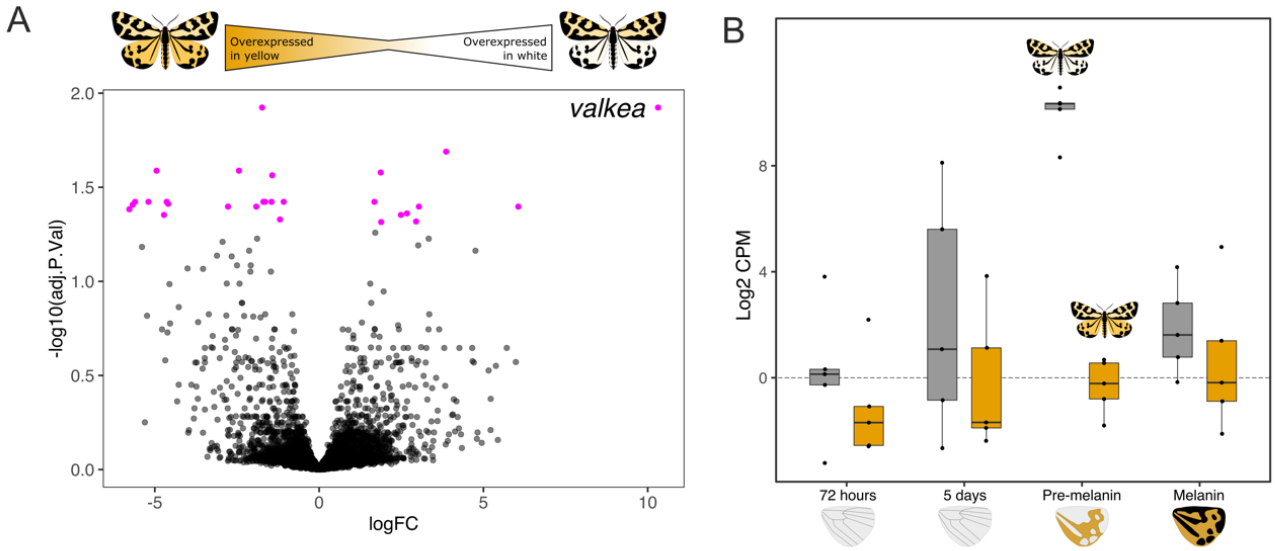

Figure 3: *Valkea* is overexpressed in white males in the pre-melanin stage. (A) In pink are genes that are significantly differentially expressed between yellow and white morphs at the pre-melanin stage. *Valkea* is the most DE gene (i.e. gene with the highest Log Fold Change). (B) Expression of *valkea* across developmental timepoints shows that it has higher expression measured in Log2 CPM (Counts Per Million) in white individuals compared to yellow ones. Expression of *valkea* in yellow morphs is around 0.

CRISPR/Cas9 knockouts of valkea produce yellow hindwings

To confirm the function of *valkea* in wing colouration, we used CRISPR/Cas9 to knock out the gene in white morphs. We tested 5 different guides to target the first 3 exons of *valkea* and injected Cas9/sgRNA duplexes into a total of 1223 eggs. Of 143 larvae that hatched only 6 developed to adults (Table S4). However, of the five males that did eclose, four had a visible change in phenotype. Males produced yellow scales instead of white on the dorsal side of both the forewings and the hindwings (Figure 4). Forewings were more yellow than in the wildtype yellow males, which usually have lighter forewings compared to hindwings. White scales on the ventral side of the wings also became yellow, similar to wildtype yellows. Black melanin patterning did not seem to be affected. Variation in the amount of melanin can be attributed to the populations from which the individuals originated, with the darker samples coming from the Finnish population (Figure 4 – figure supplement 1). Wildtype white morphs also reflect UV, particularly on the hindwings, but this is not seen in the CRISPR males (Figure 4 – figure supplement 2). This could suggest a change in scale structure, or that the yellow pigment covers the UV-reflecting structures.

Four out of the five guides tested produced a mutant phenotype, with no differences in the male phenotype between guides. The similarity of *valkea* to *yellow-e* means that it is likely that *yellow-e* could also have been knocked-out in these individuals. We used whole genome sequences of the mutants to confirm that the correct sites in *valkea* had been targeted (Figure 4 – figure supplement 3). All samples also showed evidence of editing at the corresponding *yellow-e* exons, which mainly involved insertions. The change in forewing colour could be attributed to a *yellow-e* mutation. Only one female survived to adulthood, and this had a mosaic phenotype. This individual had one yellow forewing, similar to the male mutants, with the rest of the body and wings being wildtype (Figure 4 – figure supplement 1). Since we did not expect a *valkea* knockout to affect female phenotypes as they always have red hindwings, this could be further evidence for the effect of *yellow-e* on forewing colour.

Survival of the eggs varied between the guides, although this was largely affected by the female, as hatching rate between females ranged from 0 to 70%. Females often lay unfertilised eggs so we expect that hatching rate will be low in some crosses. Using two guides in combination did not produce any pupae or adults.

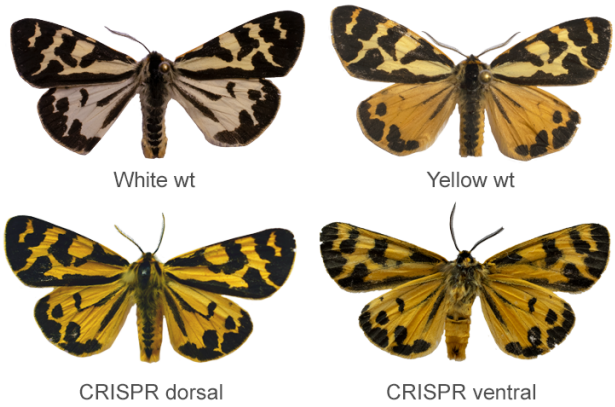

Figure 4: CRISPR/Cas9 knockouts of *valkea* transforms white scales into yellow scales across both hindwings and forewings. Wildtype WW and yy morphs (top), and the dorsal and ventral sides of one of the CRISPR knockout males (bottom).

Pigment analysis

Since the *yellow* gene family, to which *valkea* is related, is known to be responsible for the production of melanin pigments, we further investigated the identity of the wing pigmentation. First, we ruled out the presence of several non-melanin pigment types in the hindwings, including pterins and carotenoids. Pterins are commonly found in insects and, along with purine derivatives, papiliochromes and flavonoids, are soluble in strong acids and bases or in organic solvents (Umebachi, 1975; Kayser, 1985; Shamim *et al.*, 2014). We placed wing samples from each morph in NaOH overnight, then measured the absorbance of the supernatant using a spectrophotometer. We also left wings in methanol overnight before measuring the supernatant. The spectra did not show any peaks indicative of any pigment dissolved in the sample. Similarly, we found no evidence for carotenoid pigments after dissolving in a hexane:tert-butyl methyl ether solution (Appendix Figure 2). Wings did not fluoresce under UV light, providing further evidence for the lack of fluorescent pigments including pterins, flavonoids, flavins and papiliochromes (Umebachi, 1975; Kayser, 1985). Ommochromes are red and yellow pigments; high performance liquid chromatography (HPLC) ruled out the presence of these pigments on the moth wings, which we compared to data from ommochrome-containing *Heliconius* wings and a Xanthurenic acid standard (Appendix Figure 3).

HPLC analysis showed peaks characteristic of pheomelanin (Appendix Figure 4). Pheomelanins produce red-brown colour in grasshoppers and wasps (Galván *et al.*, 2015; Jorge García, Polidori and Nieves-Aldrey, 2016), and orange-red colours in ants and

277 bumblebees (Hines *et al.*, 2017; Polidori, Jorge and Ornosa, 2017). Insects generally have
278 dopamine-derived pheomelanin and a breakdown product of this is 4-Amino-3-
279 hydroxyphenylethylamine (4-AHPEA) (Barek *et al.*, 2018). Yellow wings showed large
280 peaks for 4-AHPEA. White wings had around 27% of the 4-AHPEA levels seen in yellow
281 wings, and black sections of the wings had 16%. Hydrogen iodide hydrolysis of wings
282 produced the isomer 3-AHPEA, which may come from 3-nitrotyramine originating from the
283 decarboxylation of 3-nitrotyrosine. Reduction of 3-nitrotyrosine produces 3-AHP, another
284 marker of pheomelanin (Wakamatsu, Ito and Rees, 2002).
285
286 Analysis of the black portions of the wing found pyrrole-2,3-dicarboxylic acid (PDCA) and
287 pyrrole-2,3,5-tricarboxylic acid (PTCA) (Appendix Figure 5). Both are components of
288 eumelanin (Barek *et al.*, 2018), suggesting that the black colouration seen in the wood tiger
289 moth is predominantly eumelanin derived from dopamine. This is common in producing
290 black colouration and providing structural components of the exoskeleton. In addition,
291 dopamine is acylated to both *N*-β-alanyldopamine (NBAD) and *N*-acetyldopamine (NADA)
292 sclerotins. NADA sclerotins are colourless and likely to be present on the white wings. This
293 analysis of pigmentation is therefore consistent with a role for *yellow* family genes in
294 regulating the colour polymorphism.

295 **Discussion**

296 Hindwing colouration of male *Arctia plantaginis* is polymorphic and these colour morphs
297 vary in multiple behavioural and life-history traits, providing an example of a complex
298 polymorphism. Here, we have shown that variation in male hindwing colour is associated
299 with a duplicated sequence found only in white morphs and containing a gene from the
300 *yellow* gene family. The white-specific copy, *valkea,* is highly expressed during pupal
301 development, consistent with genetic dominance of the white allele. When *valkea* is knocked
302 out in the white morphs, yellow pigment is produced, providing functional evidence that
303 *valkea* is responsible for the white phenotype rather than other genes in this region.

304 These results add to the increasing evidence for the role of gene duplications in the evolution
305 of adaptive genetic variation. Genes for the metabolisms of proteins in *Heliconius* butterflies
306 underwent several duplications, facilitating changes in diet and adaptation to pollen feeding
307 (Smith, Macias-Muñoz and Briscoe, 2016). In *Zerene cesoina* butterflies, recent partial
308 duplications of the transcription factor *doublesex,* resulting from multiple duplication events,

309 are associated with sex-specific wing patterning. The duplicated paralog acts as a repressor of
310 genes producing UV-reflecting wing scales in females (Rodriguez-Caro *et al.*, 2021).

311 We hypothesise that the morph-specific duplication that we see in *A. plantaginis* provides a
312 region of reduced recombination between morphs, as the duplicated region is effectively
313 hemizygous and cannot recombine except in homozygote genotypes, which could contribute
314 to the maintenance of the complex polymorphism and the linkage of multiple traits. This is
315 similar to the genetic architecture of the *Primula* supergene controlling heterostyly, which
316 involves a large duplication containing five genes (Huu *et al.*, 2020). In polymorphic *Papilio*
317 *dardanus*, one colour pattern morph is associated with a duplicated region, again providing
318 physical constraints on recombination (Timmermans *et al.*, 2014). Nonetheless, in the case of
319 the wood tiger moth, it remains unclear how a single gene, such as *valkea*, can control the
320 development of a broad array of phenotypic traits.

321 One possible mechanism is that there is a regulatory element along the scaffold which is
322 controlling colour via the *valkea* gene, but also regulating other genes to control different
323 phenotypic traits. We found the most significant markers and SNPs located in a non-coding
324 region close to the *yellow* genes, which likely contains a cis-regulatory element (CRE)
325 controlling transcription of *valkea.* In cichlids, for example, a CRE at the gene encoding
326 agouti-related peptide 2 controls variation in strip patterning in two closely related species
327 (Kratochwil *et al.*, 2018). Conserved CREs were shown to have wide ranging effects on wing
328 patterning in multiple Nymphalidae butterflies (Mazo-Vargas *et al.*, 2022).

329 Differential expression of other genes on the same chromosome controlled by the CRE could
330 explain variation in covarying traits. The over-expression of another gene, possibly encoding
331 a zinc transcription factor, in yellow individuals in the early pupal stages suggests that there
332 is differential expression of unlinked genes as a result of the polymorphism, although since
333 this gene is on a different chromosome to *valkea* it is unlikely to be directly controlled by the
334 CRE. Another hypothesis is that somehow *valkea* itself regulates other genes. However,
335 *yellow* family genes are not known to regulate transcription of other genes, unlike for
336 example *doublesex*, which undergoes alternative splicing and female mimetic wing pattern
337 polymorphism in *Papilio polytes* (Kunte *et al.*, 2014; Nishikawa *et al.*, 2015).

338 The *yellow* family genes are highly conserved throughout insects (Ferguson *et al.*, 2011).
339 They have been widely linked to colouration (Wittkopp, Vaccaro and Carroll, 2002;

340 Miyazaki *et al.*, 2014; Zhang *et al.*, 2017; Zhang, Mazo-Vargas and Reed, 2017), as well as
341 behaviour, sex-specific phenotypes and reproductive maturation (Wilson *et al.*, 1976). These
342 genes share a common origin with the major royal jelly protein (MRJP) genes (Drapeau *et*
343 *al.*, 2006) which are crucial in caste development in honeybees. Like the MRJP genes, *yellow*
344 genes in honeybees have diverse spatial and temporal expression patterns. As our focus in *A.*
345 *plantaginis* has been on wing tissue, we are missing expression of genes in other tissues that
346 could be linked to other traits. Thus, it is not impossible to imagine that a *yellow* gene could
347 have a similar function to a MRJP in regulating the development of a complex phenotype.
348 Recent work with *Bicyclus anynana* showed that *yellow* functions as a repressor of male
349 courtship (Connahs *et al.*, 2022). On the other hand, sex-specific behavioural phenotypes of
350 *yellow* mutants in *Drosophila* were found to be due to pigmentation effects (Massey *et al.*,
351 2019), so more evidence is needed to suggest a functional role for *yellow* genes outside of
352 pigmentation.

353 The duplication of *yellow-e* and surrounding regions in the white morphs suggests that the
354 yellow morph is the ancestral form. *Valkea* could have evolved in a stepwise fashion, first as
355 a tandem duplication then with a stop codon mutation altering the gene structure. Gene
356 duplications can facilitate adaptation and, in some examples, lead to polymorphism. The fact
357 that the white allele is dominant also supports the hypothesis that yellow is ancestral. Such
358 invasions of new adaptive alleles are facilitated when the new allele is dominant, as it is then
359 also expressed when heterozygous, i.e. the Haldane's sieve effect. Melanism, for example,
360 has repeatedly evolved in mammals due to dominant and semidominant mutations in the
361 *Mc1r* locus which have become fixed (Hoekstra, 2006).

362 *Valkea* could represent an example of neofunctionalization, where the duplicated gene gains a
363 different function to the original gene copy. In the CRISPR mutants, both forewings and
364 hindwings became yellow, and thus we suspect that *valkea* is controlling hindwing colour
365 while *yellow-e*, which was likely also knocked out due to the similarity of the sequences,
366 controls forewing colour. Those with the mutant phenotype showed only small deletions or
367 insertions around the target site. By combining multiple guides we may expect to see larger
368 deletions (Mazo-Vargas *et al.*, 2022), however none of the eggs that were injected with more
369 than one guide survived past the larval stage, suggesting that large deletions in *yellow* genes
370 reduce fitness.

371 Contrary to previous work that attributed red and yellow colours to pterins in another tiger
372 moth species (Gawne and Nijhout, 2019), we found high levels of 4-AHPEA in the yellow
373 wings confirming the presence of pheomelanins. These pigments have been widely associated
374 with red and yellow colours in mammals (e.g. Mcgraw and Wakamatsu, 2004), but only
375 relatively recently described in insects and likely to be more widespread than previously
376 thought. Yellow colours can also be produced by NBAD sclerotins which are sclerotizing
377 precursor molecules made from dopamine and these have an important role in the
378 sclerotization pathway for hardening the insect cuticle (Andersen, 2007; Barek, Evans and
379 Sugumaran, 2017) before becoming involved in melanisation (Barek *et al.*, 2018). Thus, we
380 suggest that the yellow colour arises partly from the NBAD sclerotins and partly from the
381 presence of pheomelanin pigments, which has been proposed in other Lepidoptera (Matsuoka
382 and Monteiro, 2018). While some 4-AHPEA also occurred in white wings, this may be due to
383 its role in production of cross-linking cuticular proteins and chitin during sclerotization
384 (Sugumaran, 2010). Upregulation of genes on the white allele could be acting as a repressor
385 of the generation of yellow colour. If we may speculate, *valkea* could impact the catalysis of
386 dopamine, having cascading effects down the pathway resulting in the lack of yellow
387 pigmentation. We suspect that *yellow* family genes play multiple roles within the melanin
388 production pathway. In the wood tiger moth, *yellow* affects the conversion of DOPA into
389 black dopamine melanin (Galarza, 2021). *Yellow-e* in particular has been linked to larval
390 colouration in *Bombyx mori* (Ito *et al.*, 2010) and adult colour in beetles (Wang *et al.*, 2022),
391 while another gene, *yellow-f*, has a role in eumelanin production (Barek *et al.*, 2018).

392 In summary, we identified a structural variant which is only present in white morphs of *A.*
393 *plantaginis.* This region contains a previously undescribed gene, *valkea,* which when
394 knocked out results in yellow wings. The presence of a regulatory element controlling wing
395 colour and other traits via multiple downstream effects could explain how multiple traits are
396 linked to wing colouration. This complex polymorphism allows multiple beneficial
397 phenotypes to be inherited together, whereas recombination would separate multiple loci
398 leading to maladapted individuals. Our results provide the basis for further exploration of the
399 genetic basis of covarying behavioural and life-history traits, and offer an intriguing example
400 for the role of gene duplications in adaptive variation.

401

402

403 **Methods**

404 *Sampling*

405 Homozygous lines of white (WW) and yellow (yy) *Arctia plantaginis* moths were created
406 from Finnish populations at the University of Jyväskylä, Finland. Larvae were fed with wild
407 dandelion (*Taraxacum sp*.) and reared under natural light conditions, with an average day
408 temperature of 25ºC and night temperature between 15-20ºC. For the crosses, a heterozygous
409 male, created from crossing a heterozygous male with a homozygous yy female, was
410 backcrossed with a yy female. This was repeated to obtain four families totalling 172
411 offspring and 8 parents (Table S5). Samples from wild populations were caught in Southern
412 Finland (n=10) and Central Finland (n=20), where male morphs are either white or yellow,
413 Estonia (n=4), where males are mostly white, and Scotland (n=4), where males are yellow
414 (Table S6). In addition, we included 8 samples which are F1 offspring of wild Scottish
415 samples. Forty pupae with known genotypes from lab populations (20 WW and 20 yy) were
416 used for the RNA extractions.

417 *DNA extraction and sequencing*

418 For the lab crosses, DNA was extracted from two legs crushed with sterilised PVC pestles
419 using a Qiagen DNeasy Blood & Tissue kit, following the manufacturer's instructions.
420 Library preparation and GBS sequencing were performed by BGI Genomics on an Illumina
421 HiSeq X Ten. For the wild samples, DNA was extracted from the thoraces also with a Qiagen
422 kit. Library preparation and sequencing were performed by Novogene (Hong Kong, China).
423 150bp paired-end reads were sequenced on an Illumina NovaSeq 6000 platform.

424 *Linkage mapping analysis*

425 FASTQ reads were mapped using bowtie v2.3.2 (Langmead and Salzberg, 2012) to the
426 yellow *Arctia plantaginis* scaffold-level genome assembly (Yen *et al.*, 2020). BAM files
427 were sorted and indexed using SAMtools v.1.9 (Li *et al.*, 2009) and duplicates removed using
428 PicardTools MarkDuplicates (broadinstitute.github.io/picard). Twelve samples which had
429 aligned <30% were removed. Reads of the remaining samples had an average alignment of
430 94%. SNPs were called using SAMtools mpileup with minimum mapping quality set to 20
431 and bcftools call function. Lep-MAP3 (Rastas, 2017) was used for linkage map construction
432 and we ran the following modules: ParentCall2 which called 105,622 markers, Filtering2,

433 SeparateChromosomes2 with lodLimit=5 and sizeLimit=100, JoinSingles2All and
434 OrderMarkers2 with recombination2=0 to denote the lack of female recombination.
435 Genotypes were phased using the map2genotypes.awk script included with Lep-MAP3.
436 Markers were named based on the genomic positions of the SNPs in the reference genome
437 and the map.awk script, and this was used to further order the markers within the linkage
438 groups. This resolved 30 linkage groups. Although we expect that there are 31 chromosomes
439 in the moth genome, we suspect that the sex chromosome is missing in this assembly as the
440 yy individual used in the genome assembly was female (Yen *et al.*, 2020). A small number of
441 markers which caused long gaps at the beginning or end of linkage groups were manually
442 removed, leaving the final map 948.7cM long with 19,803 markers. Markers were well
443 distributed so we began the first analyses with this map. A linkage map was also assembled
444 using sequences aligned to the white reference and this separated into 31 linkage groups.

445 The QTL analysis was carried out in R/qtl (Broman *et al.*, 2003). Genotype probabilities were
446 calculated before running a genome scan using the *scanone* function with the Haley-Knott
447 method and binary model parameters, and including family as an additive covariate. The
448 phenotype was labelled as either 0 (Wy) or 1 (yy). We ran 5000 permutations to determine
449 the significance level for the QTL LOD scores. The *bayesint* function calculated the 95%
450 Bayesian confidence intervals around the significant marker.

451 *Analysis of whole genome sequences*

452 FASTQ reads were mapped to the yellow *A. plantaginis* genome assembly (Yen *et al.*, 2020)
453 using BWA-MEM v7.17 (Li, 2013). As before, BAM files were sorted and indexed, and
454 duplicates were removed. Genotyping and variant calling was carried out with the Genome
455 Analysis Toolkit (GATK) (McKenna *et al.*, 2010). Variants were called using
456 HaplotypeCaller (v.3.7) in GVCF mode, then gVCFs combined with GenomicsDBImport
457 (v.4.0). Joint genotyping was run with GenotypeGVCFs, set with a heterozygosity of 0.01,
458 and SNPs were called using SelectVariants. Finally, the set of 20,787,772 raw SNPs were
459 filtered using VariantFiltration and thresholds: quality by depth (QD > 2.0), root mean square
460 mapping quality (MQ > 50.0), mapping quality rank sum test (MQRankSum > −12.5), read
461 position rank sum test (ReadPosRankSum > −8.0), Fisher strand bias (FS < 60.0), and strand
462 odds ratio (SOR < 3.0). A set of 5,227,288 SNPs passed the filtering.

463 We carried out a Genome Wide Association Study (GWAS) using the R package GenABEL
464 v.1.8 (Aulchenko *et al.*, 2007). The set of filtered SNPs were converted to BED format with
465 PLINK2, keeping only biallelic SNPs (cog-genomics.org/plink/2.0/). Sites which were not in
466 Hardy-Weinberg equilibrium ($p<0.01$), or had a call rate of <0.5, were excluded. Following
467 this, 381,266 sites were retained across 40 individuals (out of 57). To account for population
468 stratification, we performed multidimensional scaling on kinship and identity-by-state (IBS)
469 information estimated from the data, and included this as a covariate in the association test.
470 Significance levels were calculated using Bonferroni corrected thresholds to account for
471 multiple testing. Central and Southern Finnish populations were pooled for this analysis,
472 based on a previous principal component analysis of these samples (Yen *et al.*, 2020).

473 In Yen et al. (2020), many of these samples were processed in the same way but aligned to
474 the white genome assembly (based on a white individual). Read depth of the W-mapped
475 samples was calculated in 1kb windows across the candidate region using BEDtools
476 (v.2.20.1) multicov (Quinlan and Hall, 2010). For visualisation, lines were smoothed using
477 LOESS and span=0.01 within ggplot2.

478 For analysis of structural variants, sequences from the white and yellow genome assemblies
479 were aligned using MAFFT v7.450 (Katoh and Standley, 2013) and viewed with Geneious.
480 Our focal sequence, scaffold 419 in the white genome, is the reverse complement of scaffold
481 206 in the yellow genome.

482 *Identification of candidate genes and tree construction*

483 To identify candidate genes in the QTL interval and GWAS region, we ran a protein
484 BLASTP v.2.4.0 search to identify *Heliconius melpomene* (Hmel2.5) proteins homologous to
485 predicted *A. plantaginis* proteins in the region from the genome annotation. Informative gene
486 names were obtained by performing a BLASTP search with the *H. melpomene* proteins
487 against all *Drosophila melanogaster* proteins in FlyBase v.FB2020_01 (flybase.org/blast).

488 For the *yellow* gene tree, we used Lepbase (Challi *et al.*, 2016) to search for *yellow* genes in
489 *Bombyx mori* (ASM15162v1). We identified *yellow-e* in *H. melpomene* by searching for
490 major royal jelly proteins, then comparing protein sequences of these against *Drosophila*
491 proteins in Flybase. The sequence for *Dmel yellow-e* was downloaded from Flybase. To make
492 the tree, coding sequences of all genes were aligned in Geneious using MAFFT v7.450

493 (Katoh and Standley, 2013), then the tree was constructed with PhyML using 10 bootstraps
494 (Guindon *et al.*, 2010).

495 *Differential gene expression*

496 We dissected the wings out of the pupae in Cambridge, UK. Pupae and larvae were sent to
497 Cambridge from Jyväskylä and were kept between 22 and 30˚C. Pupae were sexed and only
498 males were used. Dissections were made at 4 different stages: 72 hours after pupation (72h),
499 5 days after pupation (5d; counting 0-24 first hours after pupation as day 1), pre melanin
500 deposition (Pre-mel) and post melanin deposition (Mel). We sampled 5 individuals per stage
501 and genotype. Hindwings and forewings were stored separately in RNA-later (Sigma-
502 Aldrich) at 4 ˚C for 2 weeks and later transferred to -20 ˚C, while the rest of the body was
503 stored in pure ethanol. Only hindwings were used for RNAseq analysis.

504 Total RNA was extracted from hindwing tissue using a standard hybrid protocol. First, we
505 transferred the wing tissue into Trizol Reagent (Invitrogen) and homogenised it using dounce
506 tissue grinders (Sigma-Aldrich). Then, we performed a chloroform phase extraction, followed
507 by DNase treatment (Ambion) for 30 mins at 37˚C. We measured the concentration of total
508 RNA using Qubit Fluorometric Quantitation (Thermofisher) and performed a quality check
509 using an Agilent 4200 TapeStation (Agilent). The extracted total RNA was stored at -20˚C
510 before being sent to Novogene UK for sequencing. Each individual was sequenced
511 separately, with a total of 40 individual samples sequenced (5 individuals per stage and
512 genotype).

513 We performed quality control and low-quality base and adapter trimming of the sequence
514 data using *TrimGalore!* We then mapped the trimmed reads to the two *A. plantaginis*
515 genomes using STAR (Dobin *et al.*, 2013). We performed a second round of mapping (2pass)
516 including as input the output splice junctions from the first round. The *A. plantaginis* genome
517 annotations WW and YY were included in each round of mapping respectively. We then used
518 *FeatureCounts* to count the mapped reads. Finally, we used DESeq2 to analyse the counts
519 and perform the DE analysis.

520 To identify the gene or genes controlling the development of wing colour in *A. plantaginis*,
521 we performed a genome wide differential expression analysis using limma-voom (Ritchie *et*
522 *al.*, 2015). First, we defined a categorical variable, 'GenStage', with 8 levels containing the
523 genotype and stage information of every individual sample (e.g. YY72h, WW72h, YY5days,

524 etc.). Then, we built the design matrix fitting a model with GenStage as the only fixed effect
525 factor contributing to the variance in gene expression and included family as a random effect
526 factor (gene expression ~ 0 + GenStage + (1|Family)). We then filtered lowly expressed
527 genes using the filterByExpr function in limma, which resulted in a reduction of the number
528 of tested genes from 17,615 to 11,330 genes in the Y-mapped analysis and 17,930 to 10,920
529 in the W-mapped one. Then, we normalised the expression of the genes using the
530 calcNormFactors function with TMM normalisation in limma and fit the design matrix using
531 the voom function. We built a contrast matrix including the comparisons of interest, in which
532 we compared the expression of the genotypes in each stage (i.e. h72=WW72h-YY72h,
533 d5=WWd5-YYd5, Premel=WWPremel-YYPremel, Mel=WWMel-YYMel), and fit the
534 contrast matrix to the data using the contrasts.fit function. Finally, we used the eBayer
535 function on the fit dataset and we extracted the list of genes that are differentially expressed
536 in each stage using the Benjamini-Hochberg procedure to correct for multiple testing. We
537 evaluated the genome wide gene expression using multidimensional scaling (MDS) using the
538 plotMDS function of the limma package.

539 *Orthology assignment*

540 To infer genome wide orthology between *A. plantaginis* and *D. melanogaster*, we used
541 OrthoFinder (v2.5.4) (Emms and Kelly, 2019). We used proteomes from six Lepidoptera
542 species, *Plutela xylostella* (GCA_905116875_2), *Bombyx mori* (GCF_014905235_1),
543 *Spodoptera frugiperda* (GCF_011064685_1), *Parnassius apollo* (GCA_907164705_1),
544 *Pieris macdunnoughi* (GCA_905332375_1) and *Pararge aegeria* (GCF_905163445_1) and
545 *Drosophila melanogaster* (GCF_000001215_4). We ran the primary_transcript.py utility
546 from OrthoFinder to extract only one transcript per protein, and then ran OrthoFinder with
547 default settings.

548 *CRISPR/Cas9 genome editing*

549 Guide RNAs were designed within the first 3 exons of *valkea* in the white genome annotation
550 using Geneious (v. 2022.1.1). Guides were chosen with minimal off-target effects, high
551 activity scores and high specificity scores based on the Geneious algorithm (Table S7).
552 Guides in the first two exons of *valkea* showed off-target sites in *yellow-e*, however those in
553 exon 3 showed no off-target sites. Guide RNAs were synthesised by Sigma-Aldrich. Moths
554 from the greenhouse populations, originating from Finnish and Estonian populations, at the

555 University of Helsinki, Finland, were genotyped using DNA extracted from leg tissue using
556 the Chemagic DNA tissue kit (Chemagen) and the primers detailed below. They were paired
557 and left to mate overnight. Females were watched over the next 3-4 days for egg laying, and
558 the eggs were removed and injected less than 6 hours after laying. Eggs were glued to
559 microscope slides and injected with a 1:1 sgRNA/Cas9 mix with phenol red dye using pulled
560 borosilicate glass capillaries. The injection mix contained 1ug/ul Cas9, 500ng/ul sgRNA and
561 0.5% phenol red. Guides and Cas9 were diluted using low concentration TE buffer. Different
562 combinations of guides were also injected in some samples, in which case these were mixed
563 in a 1:1 ratio. Injections were performed using a MPPI-3 pressure injector with back pressure
564 unit (ASI). In total, we injected 1223 eggs from 18 [WW x WW] or [WW x Wy] crosses.
565 Larvae were kept individually in petri dishes and fed daily with dandelion leaves. After
566 eclosion, legs were taken from adults for DNA extraction. Library preparation and whole
567 genome sequencing (using Illumina NovaSeq 6000) of 5 CRISPR mutants was performed by
568 CeGaT (Tübingen, Germany).

569 *Genotyping white and yellow alleles*

570 We used Primer3 to design primers within the duplicated region. Primers were expected to
571 only amplify in WW and Wy individuals. The alignment of the white and yellow sequences
572 was then used to design primers for genotyping the locus (Table S2). We looked for short
573 insertions or deletions that were fixed between the WW and yy within the *valkea/yellow-e*
574 region, and put primers around these structural variants. Primers were tested on DNA
575 extractions from moths of known genotypes, including both sexes, wild and lab samples. We
576 used Sanger sequencing of the PCR product to confirm the correct sequences were
577 amplified. A set of primers successfully amplified a 449bp region downstream of *valkea*
578 within the duplication. This amplified in WW and Wy samples, but not in yy (Appendix
579 Figure 1). We found that white alleles have a 35bp deletion within an intron of the *yellow-e*
580 gene. We amplified a 163bp region around this (YY_tarseq_206_arrow:9,846,212-9,846,375)
581 using a standard PCR protocol which allowed us to identify the allele based on the size of the
582 PCR product. Yellow alleles produce the full 163bp sequence, while white alleles produce a
583 smaller 128bp product (Appendix Figure 1). Heterozygotes have a copy of each and show
584 both bands on a gel.

585

586 *Pigment analysis*

587 Solubility and fluorescence tests

588 Five hindwings from each morph were placed in two separate solvents (0.1M NaOH and 90%
589 MeOH) and left overnight. The supernatant was analysed with an Agilent Cary 8454 UV-
590 Visible spectrophotometer and the spectra compared to known spectra for various pigments.
591 A UV lamp (Philips TL8W/08 F8T5/BLB) was used to test for fluorescence on the wings.
592 The presence of carotenoids was tested by placing wings into 1ml of pyridine and leaving at
593 95ºC for 4 hours (McGraw *et al.*, 2002). To these we added 1ml of 1:1 hexane:tert-butyl
594 methyl ether and 2ml of water before shaking and leaving overnight. Again, the supernatant
595 was measured with the spectrometer.

596 High-Performance Liquid Chromatography (HPLC) to test to for eumelanin and
597 ommochrome pigments

598 To determine the type of melanin producing the black colour on the wings, we cut out
599 approximately 5mg of the black sections of the wings, from both females and males.
600 Eumelanin analysis was carried out according to (Borges *et al.*, 2001). Each sample was
601 added to a tube containing 820µl 0.5 M NaOH, 80µl 3% H_2O_2 and an internal standard
602 (48nmol phthalic acid) and heated in a boiling water bath for 20 minutes. Once cool, 20µl of
603 10% Na_2SO_3 and 250µl of 6M HCl were added. Samples were then extracted twice with 7ml
604 of ethyl acetate. Ethyl acetate was dried at 45 °C under a stream of nitrogen. The residue was
605 dissolved into 0.5ml of 0.1% formic acid.

606 We carried out high-performance liquid chromatography on an Agilent 1100 HPLC. 20µl of
607 the sample was injected into a Waters Atlantis T3, 100 x 3.0mm i.d. analytical column
608 (Waters, Milford, MA, USA). The column was set to 25°C and analytes were detected at
609 wavelength 280nm. The HPLC mobile phase consisted of two eluents: UHQ-water/MeOH
610 (98/2; v/v) with 0.1% formic acid and UHQ-water/MeOH (40/60; v/v) with 0.1% formic acid.
611 Flow rate was 0.4 ml/min and the used gradient started with 100% of eluent A and ramped
612 evenly from time 0 to 15 minutes to 40:60 (A:B; v/v), held at 40:60 for 6 minutes and ramped
613 evenly back to initial eluent composition (100% A) over 5 minutes. We compared
614 chromatograms obtained from the samples to the chromatograms obtained from synthetic
615 melanin, ink from sepia officinalis and black human hair.

616 HPLC was also applied to observe the possible presence of ommochrome pigments. Injection
617 volume was 10µl and for the separation we used the same Waters Atlantis T3 column (100 x
618 3.0 mm i.d.) set to 30°C. Solvent A was UHQ-water and B was acetonitrile (ACN), both
619 containing 0.1% formic acid. Flow rate was 0.4ml/min and the used gradient was as follows:
620 Initial flow ratio was 98/2 water/ACN (v/v) ramping then evenly from time 1 to 15 min to
621 30:70 water:ACN (v/v), held for 1.5 min and then ramped evenly back to initial eluent
622 composition over 0.5 minutes. The column was stabilised for 7 minutes before a new run.

623 Pheomelanin analysis

624 Samples were analysed for pheomelanin content according to the method of Kolb *et al.*
625 (1997) with modifications. A 2mg sample was placed in a screw-capped tube with 100µl
626 water, 500µl ~55-58% hydrogen iodide (HI), and 20µl 50% hypophosphorous acid (H_3PO_2).
627 Samples were capped tightly and hydrolysed for 20 hours at 130°. After cooling, samples
628 were evaporated under nitrogen flow, then dissolved in 1ml of 0.1M HCl and purified with
629 solid phase extraction. Strata SCX cartridges were preconditioned with 2ml of methanol, 3ml
630 of water and 1ml of 0.1M HCl. Sample was then applied to the cartridge, washed with 1ml of
631 0.1M HCl, and finally eluted with 1ml of methanol (MeOH): 0.5M ammonium acetate
632 ($NH_4CH_3CO_2$) (20:80 v/v).

633 Hydrogen Iodide hydrolysis products were determined by a Dionex high-performance liquid
634 chromatograph equipped with pulsed amperometric detection (HPLC/PAD). A Phenomenex
635 Kinetex C18 column (150 x 4.6 mm i.d.; 5µm particle size) with a gradient elution (Table S8)
636 at a flow rate of 0.9 ml min^{-1} with the eluents: (A) sodium citrate buffer (Hines *et al.*, 2017)
637 in ultra-high-quality water (internal resistance ≥ 18.2 MΩ cm; Milli-Q Plus; Millipore,
638 Bedford, MA, USA) and (B) methanol were used for the separation. Dionex ED-50 pulsed
639 amperometric detector (Dionex, Sunnyvale, CA, USA) equipped with a disposable working
640 electrode by using a Dionex waveform A with potentials presented in Table S9 was used for
641 detection. The preparation method for the 4-AHP, 3-AHPEA and 4-AHPEA standards used
642 in calibration is described in (Wakamatsu *et al.*, 2014).

643 **Acknowledgements**

644 We thank Alma Oksanen, Kaisa Suisto and the greenhouse staff for insect rearing, and Elisa
645 Salmivirta and Sari Viinikainen for lab assistance. Thanks to Emeritus Prof. Shosuke Ito for
646 kindly providing pheomelanin standards, and to Bodo Wilts for advice on the pigment

647 analyses. We thank Muktai Kuwalekar, Claudius Kratochwil, Rachel Blow, Ian Warren, Tom
648 Generalovic and Joe Hanly for providing equipment and advice regarding the CRISPR
649 injections.

650 **Funding**

651 This work was supported by Academy of Finland grants to MB (#343356) and JM (projects
652 345091 and 328474).

653 **Data availability**

654 Scripts and data for the QTL, GWAS and DE analyses can be found at
655 doi:10.5281/zenodo.6560628. RADseq, RNAseq data, and WGS of CRISPR samples were
656 deposited to SRA under study accession number PRJNA937225. Raw sequencing data of
657 wild samples has previously been deposited in ENA, study accession No. PRJEB36595.

658

659 **References**

660 Andersen, S. O. (2007) 'Involvement of tyrosine residues, N-terminal amino acids, and β-
661 alanine in insect cuticular sclerotization', *Insect Biochemistry and Molecular Biology*, 37(9),
662 pp. 969–974. doi: https://doi.org/10.1016/j.ibmb.2007.05.002.

663 Andrade, P. *et al.* (2019) 'Regulatory changes in pterin and carotenoid genes underlie
664 balanced color polymorphisms in the wall lizard', *Proceedings of the National Academy of*
665 *Sciences of the United States of America*, 116(12), pp. 5633–5642. doi:
666 10.1073/pnas.1820320116.

667 Aulchenko, Y. S. *et al.* (2007) 'GenABEL: an R library for genome-wide association
668 analysis', *Bioinformatics*, 23(10), pp. 1294–1296. doi: 10.1093/bioinformatics/btm108.

669 Barek, H. *et al.* (2018) 'Insect cuticular melanins are distinctly different from those of
670 mammalian epidermal melanins', *Pigment Cell and Melanoma Research*, 31(3), pp. 384–392.
671 doi: 10.1111/pcmr.12672.

672 Barek, H., Evans, J. and Sugumaran, M. (2017) 'Unraveling complex molecular
673 transformations of N-β-alanyldopamine that account for brown coloration of insect cuticle',
674 *Rapid Communications in Mass Spectrometry*, 31(16), pp. 1363–1373. doi:
675 https://doi.org/10.1002/rcm.7914.

676 Borges, C. R. *et al.* (2001) 'Relationship of Melanin Degradation Products to Actual Melanin
677 Content: Application to Human Hair', *Analytical Biochemistry*, 290(1), pp. 116–125. doi:
678 https://doi.org/10.1006/abio.2000.4976.

679 Briolat, E. S. *et al.* (2019) 'Diversity in warning coloration: selective paradox or the norm?',
680 *Biological Reviews*, 94(2), pp. 388–414. doi: 10.1111/brv.12460.

681 Broman, K. W. *et al.* (2003) 'R/qtl: QTL mapping in experimental crosses', *Bioinformatics*,
682 19(7), pp. 889–890. doi: 10.1093/bioinformatics/btg112.

683 Challi, R. J. *et al.* (2016) 'Lepbase: the Lepidopteran genome database', *bioRxiv*, p. 56994.
684 doi: 10.1101/056994.

685 Connahs, H. *et al.* (2022) 'The yellow gene regulates behavioural plasticity by repressing
686 male courtship in Bicyclus anynana butterflies', *Proceedings of the Royal Society B:*
687 *Biological Sciences*, 289(1972), p. 20212665. doi: 10.1098/rspb.2021.2665.

688 Cott, H. B. (1940) *Adaptive coloration in animals*. London: Methuen.

689 Cuthill, I. C. *et al.* (2017) 'The biology of color', *Science*, 357(6350). doi:
690 10.1126/science.aan0221.

691 Dobin, A. *et al.* (2013) 'STAR: ultrafast universal RNA-seq aligner', *Bioinformatics*, 29(1),
692 pp. 15–21. doi: 10.1093/bioinformatics/bts635.

693 Drapeau, M. D. *et al.* (2006) 'Evolution of the Yellow/Major Royal Jelly Protein family and
694 the emergence of social behavior in honey bees', *Genome Research*, 16(11), pp. 1385–1394.
695 doi: 10.1101/gr.5012006.

696 Emms, D. M. and Kelly, S. (2019) 'OrthoFinder: phylogenetic orthology inference for
697 comparative genomics', *Genome Biology*, 20(1), p. 238. doi: 10.1186/s13059-019-1832-y.

698 Endler, J. A. (1988) 'Frequency-dependent predation, crypsis and aposematic coloration',
699 *Philosophical Transactions of the Royal Society B: Biological Sciences*, 319, pp. 505–523.

700 Ferguson, L. C. *et al.* (2011) 'Evolution of the insect yellow gene family', *Molecular Biology*
701 *and Evolution*, 28(1), pp. 257–272. doi: 10.1093/molbev/msq192.

702 Funk, E. R. *et al.* (2021) 'A supergene underlies linked variation in color and morphology in
703 a Holarctic songbird', *Nature Communications*, 12(1), p. 6833. doi: 10.1038/s41467-021-
704 27173-z.

705 Galarza, J. A. *et al.* (2014) 'Temporal relationship between genetic and warning signal
706 variation in the aposematic wood tiger moth (Parasemia plantaginis)', *Molecular Ecology*,
707 23(20), pp. 4939–4957. doi: 10.1111/mec.12913.

708 Galarza, J. A. (2021) 'Comparative transcriptomics of albino and warningly-coloured
709 caterpillars', *Ecology and Evolution*, 11(12), pp. 7507–7517. doi:
710 https://doi.org/10.1002/ece3.7581.

711 Galván, I. *et al.* (2015) 'Insects synthesize pheomelanin', *Pigment Cell and Melanoma*
712 *Research*, 28(5), pp. 599–602. doi: 10.1111/pcmr.12397.

713 Gawne, R. and Nijhout, H. F. (2019) 'Expanding the nymphalid groundplan's domain of
714 applicability: pattern homologies in an arctiid moth (Utetheisa ornatrix)', *Biological Journal*
715 *of the Linnean Society*, 126(4), pp. 912–924. doi: 10.1093/biolinnean/bly193.

716 Gordon, S. P. *et al.* (2015) 'Colour polymorphism torn apart by opposing positive frequency-
717 dependent selection, yet maintained in space', *Journal of Animal Ecology*, 84(6), pp. 1555–
718 1564. doi: 10.1111/1365-2656.12416.

719 Guindon, S. *et al.* (2010) 'New Algorithms and Methods to Estimate Maximum-Likelihood
720 Phylogenies: Assessing the Performance of PhyML 3.0', *Systematic Biology*, 59(3), pp. 307–
721 321. doi: 10.1093/sysbio/syq010.

722 Hegna, R. H., Galarza, J. A. and Mappes, J. (2015) 'Global phylogeography and geographical
723 variation in warning coloration of the wood tiger moth (Parasemia plantaginis)', *Journal of*
724 *Biogeography*, 42(8), pp. 1469–1481. doi: 10.1111/jbi.12513.

725 Hines, H. M. *et al.* (2017) 'Melanic variation underlies aposematic color variation in two
726 hymenopteran mimicry systems', *PLoS ONE*, 12(7), pp. 1–17. doi:
727 10.1371/journal.pone.0182135.

728 Hoekstra, H. E. (2006) 'Genetics, development and evolution of adaptive pigmentation in
729 vertebrates', *Heredity*, 97(3), pp. 222–234. doi: 10.1038/sj.hdy.6800861.

730 Huu, C. N. *et al.* (2020) 'Supergene evolution via stepwise duplications and
731 neofunctionalization of a floral-organ identity gene', *Proceedings of the National Academy of*
732 *Sciences of the United States of America*, 117(37), pp. 23148–23157. doi:
733 10.1073/pnas.2006296117.

734 Huxley, J. (1955) 'Morphism and evolution', *Heredity*, 9(1), pp. 1–52. doi:
735 10.1038/hdy.1955.1.

736 Ito, K. *et al.* (2010) 'Yellow-e determines the color pattern of larval head and tail spots of the
737 silkworm Bombyx mori', *Journal of Biological Chemistry*, 285(8), pp. 5624–5629. doi:
738 10.1074/jbc.M109.035741.

739 Jorge García, A., Polidori, C. and Nieves-Aldrey, J. L. (2016) 'Pheomelanin in the secondary
740 sexual characters of male parasitoid wasps (Hymenoptera: Pteromalidae)', *Arthropod*
741 *Structure & Development*, 45(4), pp. 311–319. doi: https://doi.org/10.1016/j.asd.2016.05.001.

742 Joron, M. *et al.* (2011) 'Chromosomal rearrangements maintain a polymorphic supergene
743 controlling butterfly mimicry', *Nature*, 477(7363), pp. 203–206. doi: 10.1038/nature10341.

744 Katoh, K. and Standley, D. M. (2013) 'MAFFT Multiple Sequence Alignment Software
745 Version 7: Improvements in Performance and Usability', *Molecular Biology and Evolution*,
746 30(4), pp. 772–780. doi: 10.1093/molbev/mst010.

747 Kayser, H. (1985) 'Pigments', in Kerkut, G. A. and Gilbert, L. I. (eds) *Comparative Insect*
748 *Physiology, Biochemistry, and Pharmacology*. Oxford: Pergamon Press, pp. 367–415.

749 Kolb, A. M. *et al.* (1997) 'Determination of Pheomelanin by Measurement of
750 Aminohydroxyphenylalanine Isomers with High-Performance Liquid Chromatography',
751 *Analytical Biochemistry*, 252(2), pp. 293–298. doi: https://doi.org/10.1006/abio.1997.2342.

752 Kratochwil, C. *et al.* (2018) 'Agouti-related peptide 2 facilitates convergent evolution of
753 stripe patterns across cichlid fish radiations', *Science*, 362(6413), pp. 457–460. doi:
754 10.1126/science.aao6809.

755 Kunte, K. *et al.* (2014) 'doublesex is a mimicry supergene', *Nature*, 507(7491), pp. 229–232.
756 doi: 10.1038/nature13112.

757 Küpper, C. *et al.* (2016) 'A supergene determines highly divergent male reproductive morphs
758 in the ruff', *Nature Genetics*, 48(1), pp. 79–83. doi: 10.1038/ng.3443.

759 Langmead, B. and Salzberg, S. L. (2012) 'Fast gapped-read alignment with Bowtie 2',
760 *Nature Methods*, 9, p. 357. Available at: http://dx.doi.org/10.1038/nmeth.1923.

761 Li, H. *et al.* (2009) 'The Sequence Alignment/Map format and SAMtools', *Bioinformatics*,
762 25(16), pp. 2078–2079. doi: 10.1093/bioinformatics/btp352.

763 Li, H. (2013) 'Aligning sequence reads, clone sequences and assembly contigs with BWA-
764 MEM', *arXiv*, p. 1303.3997.

765 Linnen, C. R. *et al.* (2013) 'Adaptive Evolution of Multiple Traits Through Multiple
766 Mutations at a Single Gene', *Science*, 339(6125), pp. 1312–1316. doi:
767 10.1126/science.1233213.

768 Massey, J. H. *et al.* (2019) 'The yellow gene influences Drosophila male mating success
769 through sex comb melanization', *eLife*. Edited by K. VijayRaghavan and C. L. Peichel, 8, p.
770 e49388. doi: 10.7554/eLife.49388.

771 Matsuoka, Y. and Monteiro, A. (2018) 'Melanin Pathway Genes Regulate Color and
772 Morphology of Butterfly Wing Scales', *Cell Reports*, 24(1), pp. 56–65. doi:
773 10.1016/j.celrep.2018.05.092.

774 Mazo-Vargas, A. *et al.* (2022) 'Deep cis-regulatory homology of the butterfly wing pattern
775 ground plan', *Science*, 378(6617), pp. 304–308. doi: 10.1126/science.abi9407.

776 McGraw, K. J. *et al.* (2002) 'The effect of dietary carotenoid access on sexual dichromatism
777 and plumage pigment composition in the American goldfinch', *Comparative Biochemistry*
778 *and Physiology Part B: Biochemistry and Molecular Biology*, 131(2), pp. 261–269. doi:
779 https://doi.org/10.1016/S1096-4959(01)00500-0.

780 Mcgraw, K. J. and Wakamatsu, K. (2004) 'Melanin Basis of Ornamental Feather Colors in
781 Male Zebra Finches', *The Condor*, 106(3), pp. 686–690. doi: 10.1093/condor/106.3.686.

782 McKenna, A. *et al.* (2010) 'The Genome Analysis Toolkit: A MapReduce framework for
783 analyzing next-generation DNA sequencing data', *Genome Research*, 20, pp. 1297–1303.
784 doi: 10.1101/gr.107524.110.

785 McKinnon, J. S. and Pierotti, M. E. R. (2010) 'Colour polymorphism and correlated
786 characters: Genetic mechanisms and evolution', *Molecular Ecology*, 19(23), pp. 5101–5125.
787 doi: 10.1111/j.1365-294X.2010.04846.x.

788 Miyazaki, S. *et al.* (2014) 'Sexually Dimorphic Body Color Is Regulated by Sex-Specific
789 Expression of Yellow Gene in Ponerine Ant, Diacamma Sp', *PLOS ONE*, 9(3), p. e92875.
790 Available at: https://doi.org/10.1371/journal.pone.0092875.

791 Nishikawa, H. *et al.* (2015) 'A genetic mechanism for female-limited Batesian mimicry in
792 Papilio butterfly', *Nature Genetics*, 47(4), pp. 405–409. doi: 10.1038/ng.3241.

Nokelainen, O. *et al.* (2012) 'Trade-off between warning signal efficacy and mating success in the wood tiger moth', *Proceedings of the Royal Society B: Biological Sciences*, 279(1727), pp. 257–265. doi: 10.1098/rspb.2011.0880.

Nokelainen, O. *et al.* (2014) 'Changes in predator community structure shifts the efficacy of two warning signals in Arctiid moths', *Journal of Animal Ecology*, 83(3), pp. 598–605. doi: 10.1111/1365-2656.12169.

Nokelainen, O. *et al.* (2022) 'Genetic colour variation visible for predators and conspecifics is concealed from humans in a polymorphic moth', *Journal of Evolutionary Biology*, (February), pp. 467–478. doi: 10.1111/jeb.13994.

Orteu, A. and Jiggins, C. D. (2020) 'The genomics of coloration provides insights into adaptive evolution', *Nature Reviews Genetics*, 21(8), pp. 461–475. doi: 10.1038/s41576-020-0234-z.

De Pasqual, C. *et al.* (2022) 'Heterozygote advantage and pleiotropy contribute to intraspecific color trait variability', *Evolution*, pp. 2389–2403. doi: 10.1111/evo.14597.

Polidori, C., Jorge, A. and Ornosa, C. (2017) 'Eumelanin and pheomelanin are predominant pigments in bumblebee (Apidae: Bombus) pubescence', *PeerJ*, 2017(5), pp. 1–21. doi: 10.7717/peerj.3300.

Quinlan, A. R. and Hall, I. M. (2010) 'BEDTools: a flexible suite of utilities for comparing genomic features', *Bioinformatics*, 26(6), pp. 841–842. doi: 10.1093/bioinformatics/btq033.

Rastas, P. (2017) 'Lep-MAP3: robust linkage mapping even for low-coverage whole genome sequencing data', *Bioinformatics*, 33, pp. 3726–3732. doi: 10.1093/bioinformatics/btx494.

Ritchie, M. E. *et al.* (2015) 'limma powers differential expression analyses for RNA-sequencing and microarray studies', *Nucleic Acids Research*, 43(7), pp. e47–e47. doi: 10.1093/nar/gkv007.

Rodriguez-Caro, F. *et al.* (2021) 'Novel Doublesex Duplication Associated with Sexually Dimorphic Development of Dogface Butterfly Wings', *Molecular Biology and Evolution*, 38(11), pp. 5021–5033. doi: 10.1093/molbev/msab228.

Rojas, B. *et al.* (2017) 'How to fight multiple enemies: Target-specific chemical defences in an aposematic moth', *Proceedings of the Royal Society B: Biological Sciences*, 284(1863). doi: 10.1098/rspb.2017.1424.

Rojas, B., Gordon, S. P. and Mappes, J. (2015) 'Frequency-dependent flight activity in the colour polymorphic wood tiger moth', *Current Zoology*, 61(4), pp. 765–772. doi: 10.1093/czoolo/61.4.765.

Rönkä, K. *et al.* (2020) 'Geographic mosaic of selection by avian predators on hindwing warning colour in a polymorphic aposematic moth', *Ecology Letters*, 23(11), pp. 1654–1663. doi: https://doi.org/10.1111/ele.13597.

Shamim, G. *et al.* (2014) 'Biochemistry and biosynthesis of insect pigments', *European Journal of Entomology*, 111(2), pp. 149–164. doi: 10.14411/eje.2014.021.

Smith, G., Macias-Muñoz, A. and Briscoe, A. D. (2016) 'Gene Duplication and Gene Expression Changes Play a Role in the Evolution of Candidate Pollen Feeding Genes in Heliconius Butterflies', *Genome Biology and Evolution*, 8(8), pp. 2581–2596. doi: 10.1093/gbe/evw180.

Sugumaran, M. (2010) 'Chapter 5 - Chemistry of Cuticular Sclerotization', in Simpson, S. J. B. T.-A. in I. P. (ed.). Academic Press, pp. 151–209. doi: https://doi.org/10.1016/B978-0-12-381387-9.00005-1.

Suomalainen, E. (1938) 'Die erblichkeitsverhältnisse des männlichen dimorphismus bei parasemia plantaginis', *Hereditas*, 24, pp. 386–390.

Thompson, M. J. and Jiggins, C. D. (2014) 'Supergenes and their role in evolution', *Heredity*, 113(1), pp. 1–8. doi: 10.1038/hdy.2014.20.

Timmermans, M. J. T. N. *et al.* (2014) 'Comparative genomics of the mimicry switch in Papilio dardanus', *Proceedings of the Royal Society B: Biological Sciences*, 281(1787). doi: 10.1098/rspb.2014.0465.

Umebachi, Y. (1975) 'Further studies on the dopamine derivative, SN-1 derived from the yellow pigments of Papilio xuthus', *Insect Biochemistry*, 5, pp. 73–92.

Wakamatsu, K. *et al.* (2014) 'Reduction of the Nitro Group to Amine by Hydroiodic Acid to Synthesize o-Aminophenol Derivatives as Putative Degradative Markers of Neuromelanin', *Molecules* . doi: 10.3390/molecules19068039.

Wakamatsu, K., Ito, S. and Rees, J. L. (2002) 'The Usefulness of 4-Amino-3-hydroxyphenylalanine as a Specific Marker of Pheomelanin', *Pigment Cell Research*, 15(3), pp. 225–232. doi: https://doi.org/10.1034/j.1600-0749.2002.02009.x.

Wang, J. *et al.* (2013) 'A Y-like social chromosome causes alternative colony organization in fire ants', *Nature*, 493(7434), pp. 664–668. doi: 10.1038/nature11832.

Wang, P. *et al.* (2022) 'Yellow-b, -c, -e and -h are required for normal body coloration in Henosepilachna vigintioctopunctata', *Archives of Insect Biochemistry and Physiology*, 109(2), p. e21856. doi: https://doi.org/10.1002/arch.21856.

Wilson, R. *et al.* (1976) 'Behavioural pleiotropy of the yellow gene in Drosophila melanogaster', *Genetical Research*. 2009/04/14, 28(1), pp. 75–88. doi: DOI: 10.1017/S0016672300016748.

Winters, A. E. *et al.* (2021) 'Multimodal Aposematic Defenses Through the Predation Sequence', *Frontiers in Ecology and Evolution*, 9(August), pp. 1–18. doi: 10.3389/fevo.2021.657740.

Wittkopp, P. J., Vaccaro, K. and Carroll, S. B. (2002) 'Evolution of yellow gene regulation and pigmentation in Drosophila', *Current Biology*, 12(18), pp. 1547–1556. doi: 10.1016/S0960-9822(02)01113-2.

Yen, E. C. *et al.* (2020) 'A haplotype-resolved, de novo genome assembly for the wood tiger moth (Arctia plantaginis) through trio binning', *GigaScience*, 9(8), pp. 1–12. doi: 10.1093/gigascience/giaa088.

Zhang, L. *et al.* (2017) 'Genetic basis of melanin pigmentation in butterfly wings', *Genetics*, 205(4), pp. 1537–1550. doi: 10.1534/genetics.116.196451.

Zhang, L., Mazo-Vargas, A. and Reed, R. D. (2017) 'Single master regulatory gene coordinates the evolution and development of butterfly color and iridescence', *Proceedings of the National Academy of Sciences*, 114, pp. 10707–10712. doi: 10.1073/pnas.1709058114.